Taylor & Francis
Taylor & Francis Group

Automatika

Journal for Control, Measurement, Electronics, Computing and Communications

ISSN: (Print) (Online) Journal homepage: https://www.tandfonline.com/loi/taut20

Restoration of deteriorated text sections in ancient document images using a tri-level semi-adaptive thresholding technique

N. Shobha Rani, B. J. Bipin Nair, M. Chandrajith, G. Hemantha Kumar & Jaume Fortuny

To cite this article: N. Shobha Rani, B. J. Bipin Nair, M. Chandrajith, G. Hemantha Kumar & Jaume Fortuny (2022) Restoration of deteriorated text sections in ancient document images using a tri-level semi-adaptive thresholding technique, Automatika, 63:2, 378-398, DOI: 10.1080/00051144.2022.2042462

To link to this article: https://doi.org/10.1080/00051144.2022.2042462

Published online: 23 Feb 2022.

AUTOMATIKA
2022, VOL. 63, NO. 2, 378–398
https://doi.org/10.1080/00051144.2022.2042462

Restoration of deteriorated text sections in ancient document images using a tri-level semi-adaptive thresholding technique

N. Shobha Rani[a], B. J. Bipin Nair[a], M. Chandrajith[b], G. Hemantha Kumar[c] and Jaume Fortuny[d]

[a]Department of Computer Science, Amrita School of Arts and Sciences, Amrita Vishwa Vidyapeetham, Mysuru-, India; [b]Department of Computer Applications, Maharaja Institute of Technology, Mysore, India; [c]Department of Studies in Computer Science, University of Mysore, Mysore, India; [d]Observatory of Globalization, University of Barcelona, Barcelona, Spain

ABSTRACT

The proposed research aims to restore deteriorated text sections that are affected by stain markings, ink seepages and document ageing in ancient document photographs, as these challenges confront document enhancement. A tri-level semi-adaptive thresholding technique is developed in this paper to overcome the issues. The primary focus, however, is on removing deteriorations that obscure text sections. The proposed algorithm includes three levels of degradation removal as well as pre- and post-enhancement processes. In level-wise degradation removal, a global thresholding approach is used, whereas, pseudo-colouring uses local thresholding procedures. Experiments on palm leaf and DIBCO document photos reveal a decent performance in removing ink/oil stains whilst retaining obscured text sections. In DIBCO and palm leaf datasets, our system also showed its efficacy in removing common deteriorations such as uneven illumination, show throughs, discolouration and writing marks. The proposed technique directly correlates to other thresholding-based benchmark techniques producing average *F*-measure and precision of 65.73 and 93% towards DIBCO datasets and 55.24 and 94% towards palm leaf datasets. Subjective analysis shows the robustness of proposed model towards the removal of stains degradations with a qualitative score of 3 towards 45% of samples indicating degradation removal with fairly readable text.

Highlights

- This work presents a semi-adaptive binarization technique for ancient image enhancement.
- Main focus of this work is to restore obscured text sections.
- Multi-level thresholding approach is used for the removal of degradations.
- Gradient of the original image is used in the computation of reference image to detect deteriorated text sections.
- Pseudo-colouring and post-enhancement process finally transform to the enhanced image.
- DIBCO and palm leaf document samples are used for experimentations.

ARTICLE HISTORY
Received 12 September 2021
Accepted 10 February 2022

KEYWORDS
Document restoration; ink/oil stain removal; binarization technique; thresholding algorithms; ancient document images; palm leaf documents

1. Introduction

In the context of documents, digitization is the process of transforming the physical documents into a format that can be processed by a computer. The primary objective of digitization is to preserve and often disseminate the valuable information of these documents [1]. There exists a wide variety of document types, such as old books, medical reports or even handwritten music scores and ancient manuscripts, such as degraded printed, handwritten and palm leaf manuscripts. Though there exist various successful works on the digitization of ancient manuscripts, it is significant to ensure that digitized documents are readable and of good resolution which requires enhancement. The task of enhancement is very complex and would usually vary from one type of document to other types due to variety of document built-up methods. Therefore, it is necessary to carryout enhancement so that the documents are degradation free and digitally good enough to identify the relevant information and useful for extraction of data from documents. The primary purpose of this study is to enhance the digitized documents by restoring deteriorated and obscured textual contents using multi-level thresholding techniques without the knowledge of labelled data. Several research attempts on ancient document digitalization initiatives have been documented since 2004 [2]. An attempt has been made in this work to solve the issues that arise during the enhancement process of digitized ancient manuscripts. Whilst acquiring, storing, processing and

CONTACT N. Shobha Rani n.shoba1985@gmail.com Department of Computer Science, Amrita School of Arts and Sciences, Amrita Vishwa Vidyapeetham, Mysuru-570026, Karnataka, India

disseminating ancient manuscripts are all key objectives of the digitization process, restoring severely deteriorated manuscripts into visually appealing digitized forms is a necessary step in the document enhancement process.

Degradation challenges such as brittleness/cracks, contrast difficulties owing to old age and ink seepage, environmental influence, ink quality, overlapping of text with analogous textured background noise and de-acidification damages have a significant impact on ancient manuscripts. All of these factors are major challenges in the digitization of ancient manuscripts, and if they are not addressed properly, they will result in poor text quality retention after digitization. Improved text readability of ancient manuscripts, promotes accessibility, natural language processing operations and makes information retrieval faster.

To deal with various challenges that arise in the process of enhancement of deteriorated ancient documents, there is no universal binarization approach. As documents are created with their own layout and made of different material types, the degradations specific to a document would vary in terms of minute inter-grey level changes between textual and deteriorated regions. The interpretation of minute inter-grey level changes to classify textual to non-textual pixels demands a simple and effective document-specific binarization technique. On the other hand, restoration of text sections obscured by degradations from digitized ancient manuscripts is also crucial because high-precision Optical Character Recognition Systems (OCRS) demand enhanced documents to boost recognition rates [1].

Enhancement of ancient DIBCO documents is a well-researched problem in the literature and various degradations such as uneven illumination, foxing effect, ink bleed throughs on two-sided printed documents are often researched. Methods such as global or local thresholding strategies are widely employed for binarization to determine if a pixel is labelled as 0 or 1 [3–10]. Global thresholding applies a unified predicate to all the pixels in an image and whereas multiple predicates are dynamically employed in local thresholding based on the local neighbourhoods of grey level distributions [11]. It is observed that the use of a unified threshold throughout the document will not produce better results for degraded documents and on the other hand use of adaptive thresholding at the block or pixel level based on local neighbourhoods would also be time consuming and computationally intensive tasks. The idea of this investigation is to combine the efficiencies of global and local thresholding approaches and use multiple thresholds based on the degradation type to be addressed. A methodology has been developed in our research to address essential issues such as restoring text sections obscured by stains, show throughs and uneven illumination in ancient manuscripts such as DIBCO datasets and palm leaf manuscripts. In this regard, Section 2 discusses a couple of noteworthy contributions for binarization of deteriorated document images.

2. Literature review

Lipiński et al. [12] evaluate the performance of 15 different global thresholding methods for binarization of water-sensitive document images. According to the results of an experimental investigation, the Otsu approach is the best of the three top-rated techniques. To overcome non-uniform illuminations, Gupta et al. [13] use a combination of local and global thresholding approaches for binarization of DIBCO documents. The method uniformizes grey level distributions successfully and has been tested on DIBCO datasets. Later, Michalik and Okarma [14] adopted both adaptive and global thresholding techniques to binarize non-uniformly illuminated documents captured by mobile sensors. Non-stain degradations were the focus of the experiment, and testing was done on non-uniformly illuminated manuscripts. Uneven illumination difficulties in DIBCO document collections are examined in the following paper Michalik and Okarma [15]. In the analytical study, problems with uneven illumination are a major concern. Following this, Michalik and Okarma [16] used a multilayered thresholding technique to address the problem of uneven illumination in Bickley diary datasets.

According to Alexander and Kumar [17], sometimes parameter tuning in adaptive thresholding algorithms delivers the best results for deteriorated palm leaf documents. In addition, the two-step binarization strategy proposed by Krupiński et al. [18] is used to handle uneven illuminations in DIBCO and Bickley diary datasets. Gaussian Mixture Models and the Monte Carlo method for binarization are used to calculate a threshold. Specific strategies for addressing the deteriorations, such as restoring obscured text sections, are not covered in this paper.

In another work, a binarization strategy using local patches of DIBCO images is used for training neural networks called U-net by Huang et al. [19]. Later, deteriorated document image binarization method is devised by Yang and Yibing [20] for the removal of signal-dependent noise, variable illuminations, shadows, smears/smudges and low contrast regions. A nonlinear reaction-diffusion model is proposed by Zhang et al. [21] for bleed-through removal using Perona Malik equation. A parallel series splitting algorithm is devised and evaluated on DIBCO datasets for bleed-through removal.

Further, binarization of damaged paper photos is performed via the modified Sauvola approach by Kaur et al. [22] using stroke width transform to decide the label of each pixel as 0 or 1. A set of synthetic images

are employed for testing and it is observed that documents tested are non-ancient document images. In a subsequent work by Guo et al. [23], a non-linear edge conserving diffusion model is used for the binarization of text photos. The algorithm is evaluated on DIBCO datasets proving that adaptive thresholding techniques perform better compared to probabilistic model-based binarization models.

Calvo and Gallego [24] used auto-encoders for binarization of DIBCO dataset images, using thresholded documents for training. Though deep learning methods perform well, a major limitation with the model is training with ground truth images of the similar category of images. In a later work by Calvo et al. [25], pixel-wise binarization of musical documents is carried out using deep convolutional neural networks. Experiments are conducted on DIBCO, musical score documents, Persian heritage and Balinese script palm documents. Though it is a successful attempt towards DIBCO, musical score and Persian heritage documents, the performance is lagging below a correlation of less than 60% towards palm leaf manuscripts. Binarization technique for ancient document images is implemented by Saddami et al. [26] using adaptive thresholding and auto-encoders. In a different work by Feng et al. [27], a model for noise removal in degraded images uses energy function to address degradations such as smudges and uneven illumination. Consecutive attempts for enhancement of degraded document images are investigated by Zhao et al. [28] using conditional generative adversarial network using generator functions. In a work by Sehad et al. [29] for document binarization, Gabor filters are used to address the challenges in degradation removal. Later, in a work by Hangarge et al. [30], local binary patterns and cosine distance are employed as parameters for logo detection in documents and also tested for binarization.

An optimal block-based adaptive thresholding technique is propped by Xiong et al. [31] for DIBCO document binarization. Datasets experimented include printed and handwritten degraded images. Though the method produces successful outcomes, specific trials addressing restoration of under text sections in images are not addressed. In a subsequent investigation by Vo et al. [32], a deep supervised network is trained to predict the text sections in DIBCO document images. The method is dependent on reference images of datasets for training. Further, in a work by Chen and Wang [33], broken and degraded text sections are enhanced using non-local means technique and Wellner's adaptive thresholding.

Preservation of stroke connections in degraded textual sections, on the other hand, has ramifications. Mitianoudis and Papamarkos [34] propose a method for damaged handwritten and printed document binarization using Gaussian Mixture models and local co-occurrence maps. Ntirogiannis et al. [35] devise a method for binarization of degraded document images using a combination of local and global thresholding techniques. In DIBCO datasets, the approach removes non-uniform illuminations, smudges and fainted letters. The difficulties of recovering blurred text strokes are not addressed.

By studying a series of attempts made in 2013 and 2012, Wen et al. [36], Su et al. [37], Chiu et al. [38] apply thresholding methods to enhance DIBCO datasets. Otsu, Sauvola, Niblack and Kittler are examples of approaches that have been demonstrated to be effective in removing uneven illumination, smudges and smearing. Hedjam et al. [39] and Bataineh et al. [40] investigate spatial pixel relationship-based techniques for binarization of DIBCO documents using a combination of thresholding and soft computing techniques. Non-uniform illuminations and ink bleeds are successfully removed in both works. Farrahi and Cheriet [41] use a multi-scale binarization technique with adaptive thresholding on damaged historical documents. The effectiveness of this method for correcting poor connections between text strokes has been demonstrated. Also, employing a low-pass Wiener filter and a background surface approximation [42] resolves degradations such as non-uniform lighting and smearing.

The following points are noted, to the best of our knowledge, after carefully analyzing the literature.

(1) Methods such as local and global thresholding as well as soft computing-based techniques are rarely used to investigate the deterioration of obscured text sections.
(2) There is no clear analysis on the importance of text visual quality during noise removal in any research.
(3) Though deep learning algorithms have been effective at removing show through and bleed through, as well as uneven illuminations in DIBCO datasets, experiments for text restoration are yet to be shown. Also, the requirements of labelled datasets in the specific type of dataset are one of the crucial parameter that decides the efficiency of system. Though the research attempts on unsupervised adaptive neural networks are implemented, recognition efficiency towards the palm leaf manuscripts is lagging behind.
(4) The majority of the works focus on the issue of uneven illumination in DIBCO documents.
(5) Experimentation with palm leaf document image enhancement is rarely found in the literature.

Some significant works that closely align with our proposed method are summarized in Table 1.

The rest of this paper is laid out as follows: Section 3 explains how the semi-adaptive document binarization technique works. Section 4 gives the experimental

Table 1. Existing methods and observations on dominantly used techniques for binarization.

Author	Year	Techniques used	Dataset details	Degradations resolved
Lipiński et al. [12]	2020	Global thresholding	Water-sensitive papers-crops spraying	Non-uniform illumination
Gupta et al. [13]	2020	Local and global thresholding procedures	DIBCO	Non-uniform illumination, smears, smudges
Michalik and Okarma [14]	2020	Adaptive thresholding	Mobile captured images	Non-uniform illumination
Michalik and Okarma [15]	2020	Optimized adaptive thresholding	DIBCO	Non-uniform illumination
Michalik and Okarma [16]	2020	Global and local thresholding procedures	Bickley diary datasets	Uneven illumination
Alexander and Kumar [17]	2020	Local/adaptive optimization	Palm leaf	Restoration of text
Krupiński et al. [18]	2020	Gaussian mixture models and Monte Carlo simulation	DIBCO+ Bickley diary datasets	Non-uniform illumination
Huang et al. [19]	2020	Global, local UNET technique	DIBCO	Non-uniform illumination
Kaur et al. [22]	2020	Modified Sauvola approach	Damaged paper photograph	Non-uniform illumination
Guo et al. [23]	2019	Adaptive thresholding	Mobile captured text photos	Non-uniform illumination
Saddami et al. [26]	2019	Adaptive thresholding and auto-encoders	Ancient document images	Smudges-uneven illumination
Calvo et al. [24]	2017	Auto-encoder approach	DIBCO	Broken text sections
Bradley et al. [36]	2007	Adaptive binarization and soft decision method	DIBCO document images	Non-uniform illumination and noise
Bartolo et al [7]	2004	Bernsen's thresholding adaptation	DIBCO document images	Variable illumination
Kittler et al. [8]	1986	Adaptive thresholding	DIBCO document images	Spatial variation in illumination
Sauvola et al. [9]	1997	Minimum error thresholding	Sketched line drawing images Point Grey camera captured images	Pixel classification error

inferences of the proposed approach utilizing palm leaf document images and DIBCO document images, as well as a comparative research with other benchmark techniques using local and global thresholding techniques.

3. Proposed methodology

Figure 1 depicts the proposed methodology for binarization of ancient document images, as well as its levels. The technique for binarizing ancient document images includes a pre-enhancement of the input image

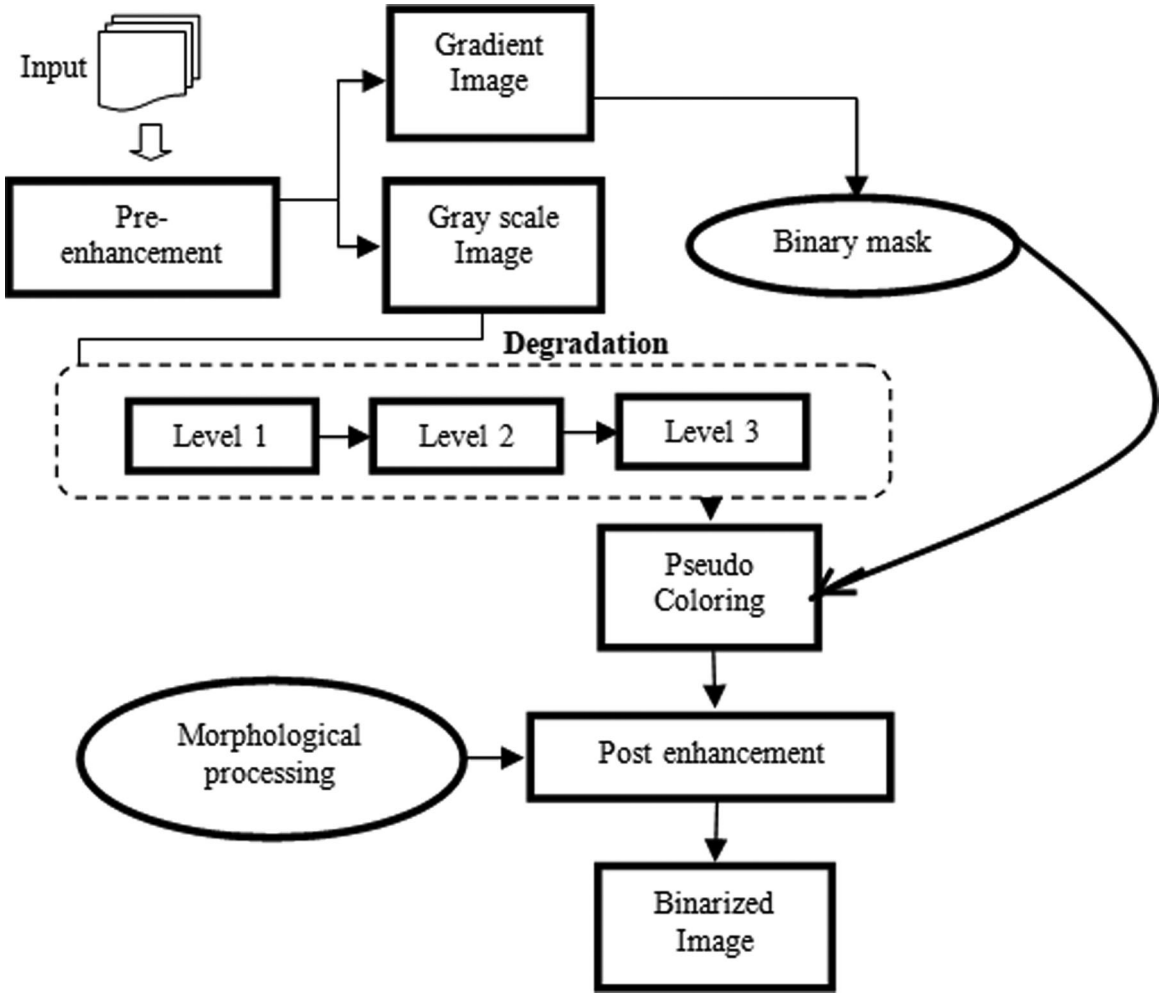

Figure 1. Block diagram of semi-adaptive binarization technique.

to apply the necessary brightness adjustments. In the next step, the image is filtered using two different workflows. In one workflow, the image is converted to grey scale, whilst in another, the image is subjected to gradient image extraction via red, green and blue channel analysis. Gradient image is used for the extraction of binary mask marking the text sections obscured by stain degradations. On the other hand, the grey-scale image obtained from the input image is subjected to mid-level processing, which includes a tri-level degradation removal process that uses statistical thresholds estimated based on the image's global grey-scale features, resulting in a tri-level noise filtered image. From that, the tri-level noise filtered image is subjected to a pseudo-colouring procedure, in which stain degradation is removed from the tri-level noise filtered image using a binary mask, resulting in a pseudo-coloured image. Finally, in post-enhancement, morphological operations are applied to the pseudo-coloured image to generate the enhanced binarized image.

3.1. Pre-enhancement

Consider an input image I for which pre-enhancement is carried out by applying contrast stretching linear function that stretches the grey level of an image I to its full dynamic range. The result of pre-enhancement is shown in Figure 2. The enhanced image I_E is the outcome of brightness modification of image I and it is used to compute the gradient image G_d, as stated subsequently.

The intensity values are modified as a result of applying the contrast stretching transformation to the input image in order to increase the discrimination between the textual pixels and the background, resulting in the restoration of slightly faded text sections as seen in Figure 2(e). Preprocessing basically turns brighter pixels into much brighter pixels, which may result in a marginal increase in noise, but it is necessary for the preservation of slightly faded text in both DIBCO and palm leaf documents. The proposed method's noise removal is effective in removing additional noise that occurs as a result of this change.

3.2. Gradient image computation

The enhanced image I_E is divided into colour channel images I_R, I_G and I_B of RGB colour space images. To compute the RGB sliced image I_d, the channel images are subjected to arithmetic processing. The computation of a gradient image is depicted in Figure 3. The average of red and blue channel images is combined with a green channel image to create an RGB sliced image I_d. The RGB sliced image is also subjected to Otsu thresholding, resulting in a binary image that serves as the reference image I_{ref}. Finally, the original image I is mapped to the reference image I_{ref}.

1. Given I_R, I_G and I_B as colour channel images of RGB image I_E
2. Arithmetic processing – RGB sliced image: $I_d \leftarrow I_G - \frac{(I_R + I_B)}{2}$
3. $I_{ref} \leftarrow$ *Otsu_Threshold* (I_d)
4. *for* $i = 1{:}r$
   for $j = 1{:}c$
   if ($I_{ref}(i, j) = \quad = 1$)
   $I(i, j, 1) = 0$;
   $I(i, j, 2) = 0$;
   $I(i, j, 3) = 0$;
   end if
   end for
   end for
5. Assignment of original image I to gradient image G_d
   $G_d = I$
6. *Stop*

Initially, the enhanced image I_E is required as input, which is separated into red I_R, green I_G and blue I_B

Figure 2. (a) Degraded image-1; (b) enhanced image of (a); (c) degraded image-2; (d) enhanced image of (c); (e) closer view of enhanced document.

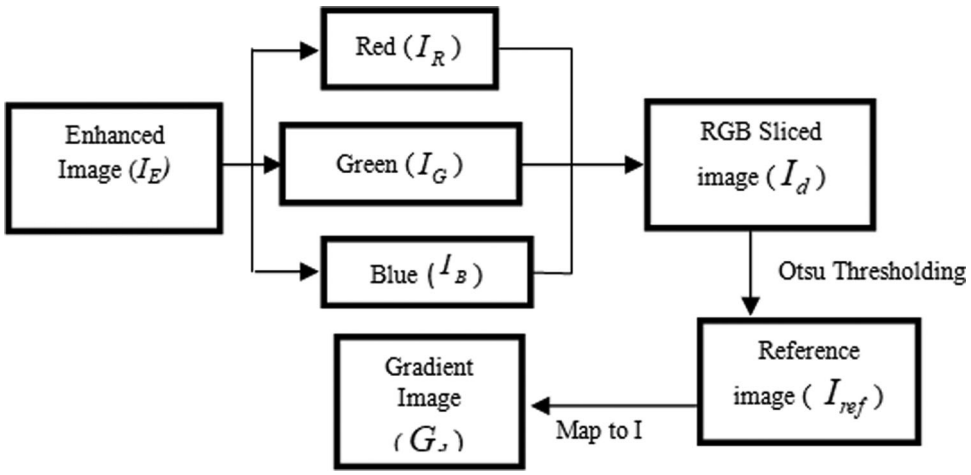

Figure 3. Computation of gradient image G_d.

channel images. The red and blue channel images are combined as I_R+I_B, divided by the number of channels used to combine, which is 2, and the result is subtracted from the green channel image I_G to generate an RGB sliced image I_d.

The overall effect of merging and dividing three channels would reduce noise, which could then be subtracted from the green channel image to aid in the detection of changes between images. In addition, deducting the combine and divide result from the green channel image contributes to the normalization of uneven text parts and the removal of shadows, yielding an RGB sliced image I_d. Following that, the RGB sliced image is subjected to Otsu's thresholding, which divides the pixels into intensity levels 0 and 1, yielding a reference image I_{ref}.

Each I_{ref} (x,y) is defined of intensities of 0 or 1 and I_{ref} (x,y) ε 0 or 1. In the reference image, a pixel I_{ref} (x, y) with intensity 1 corresponds to pixels that constitute the text sections. Each pixel $I(x, y)$ of the original image is quantized in RGB colour channel images I_R (x,y), I_G (x,y) and I_G (x,y) based on the existence of on and off pixels in the reference image. The intensity level 1 in the reference image I_{ref} is quantized with intensity level 0 in the RGB sliced image I_d for all pixels.

This technique is performed for all pixels in I_d, an M-row, n-column grid. Finally, the original image is subjected to RGB sliced image I_d mapping before being assigned as a gradient image G_d. The gradient image is vital in emphasizing the text sections that have been deteriorated and concealed.

3.3. Level 1 degradation removal

The principal objective of level 1 degradation removal is to remove the greyscale image variance caused by the

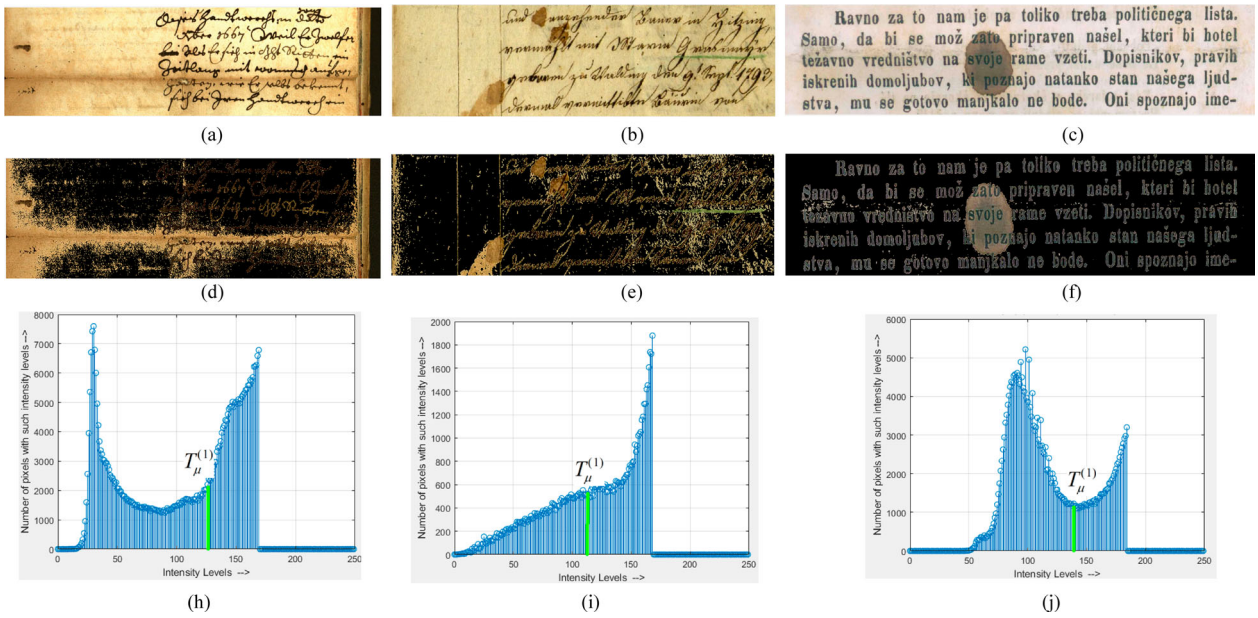

Figure 4. (a) Original image 1(I1); (b) original image (I2); (c) original image (I3); (d) gradient image-I1; (e) gradient image-I2; (f) gradient image-I3; (g) histogram-I1; (h) histogram-I2; (i) histogram-I3.

uneven lighting and shadow corrections in the source image. A transformation is applied to a greyscale that separates the grey levels over a threshold to the maximum grey level whilst keeping the grey levels below the threshold constant. The process for removing level 1 degradation is as follows.

The histogram of a gradient image is used to examine the distribution and dispersion of grey levels relating to textual and non-textual sections. To eliminate level 1 degradations, a gradient image-based threshold is applied. For categorizing grey level variations in grey-scale image G_s, the threshold is employed as a reference parameter.

Let $r_1, r_2, r_3 \ldots r_{L-1}$ be the grey levels corresponding to the gradient image G_d and ϑ is the vector holding the value $p(r_k)$ of G_d, where $k = 1, 2, 3 \ldots L-1$ and $p(r_k)$ is the probability of occurrence of a specific grey level r_k. A mean threshold $T_\mu^{(1)}$ for level 1 degradation removal is computed from trimmed vector $\overline{\vartheta}$ obtained by truncating the grey level r_k whose $p(r_k)$ is zero as given by (1).

$$T_\mu^{(1)} = \frac{1}{n} \sum\nolimits_{i \in \overline{\vartheta}} p(r_i)[G_d(:)] \tag{1}$$

In the proposed datasets for experimentation, grey levels of degradation-obscured text sections appear less dominating in brightness than the mean threshold $T_\mu^{(1)}$. Also, non-obscured background sections appear to be less prominent in brightness when it descends below the mean threshold $T_\mu^{(1)}$. Besides that, several visual perception-based implications from the proposed datasets are stated.

(1) In most of the cross-domain documents, noise constituted of grey levels below the mean threshold $T_\mu^{(1)}$ affects more than 90% of deteriorated document images.
(2) It is clear that a grey level $l(d)$ relevant to degradations such as degradation of obscured text sections, discolour-age, non-uniform lighting and ink bleed through exists between the grey levels $l(t)$ and $l(b)$ spectrum of grey levels, as illustrated in (2).

$$l(t) < l(d) < l(b) \tag{2}$$

(3) Mean threshold $T_\mu^{(1)}$ employed for level 1 degradation removal indicates the spread of grey level constant $\pm k$ of a specific grey level $l(d)$ of grey-scale image as given by (3).

$$l(d) - k \approx T_\mu^{(1)} \approx l(d) + k \tag{3}$$

The empirical relation (3) can be represented subsequently in the simplified form given by (4).

$$l(t) \approx T_\mu^{(1)} \approx l(b) \tag{4}$$

where $l(t) \approx l(d) - k, l(b) \approx l(d) + k$.

Thus, mean threshold $T_\mu^{(1)}$ is a crucial parameter in level 1 degradation removal process resulting in level 1 filtered image g_1 given by (5).

$$g_1(x, y) = 255, \; if(G_s(x, y)) \geq T_\mu^{(1)} \tag{5}$$

In the next step, level 1 filtered image g_1 is sent to level 2 degradation removal process. Figure 2 highlights the mean threshold $T_\mu^{(1)}$ obtained with the help of histograms for few instances of gradient images.

In Figure 4, mean threshold $T_\mu^{(1)}$ of I_1, I_2 and I_3 lies in the range of 110–150 indicating the degradations above the range are non-uniform illuminations, smears, smudges and foxing effect.

3.4. Level 2 degradation removal

The intention of level 2 degradation removal is to eliminate impulse and periodic noise from the level 1 filtered image g_1's output. To do so, a global threshold is calculated based on the median of the level 1 filtered image g_1. The median of the image's different grey levels is used as the filtering threshold.

For an image g_1, initially distinct grey levels $l_1, l_2, l_3 \ldots l_k$ are computed and sorted from which a median $\widetilde{g_1}$ is computed from sorted grey levels, where k is number of grey levels. The median threshold is in responsible for removing moderate and sensitive stains or blemishes on textual contents that are close to the grey levels. Let (x, y) represents an arbitrary pixel in level 1 filtered image g_1 with number of rows m and columns n, where, $x = 1, 2, 3 \ldots m, y = 1, 2, 3 \ldots n$, the median threshold $\widetilde{g_1}$ is applied on g_1 producing an outcome of level 2 filtered image g_2 as given by (6).

$$g_2(x, y) = \begin{cases} 255 & g_1(x, y) \geq \widetilde{g_1} \\ 0 & \text{Otherwise} \end{cases} \tag{6}$$

Level 2 filtered image g_2 is sent to level 3 degradation removal for the elimination of stain marks crossing text strokes.

3.5. Level 3 degradation removal

Level 3 degradation removal attempts to remove noise from degradation-obscured text sections, and uses an intensity level slicing technique to detect the range of grey levels associated with degradations. The input of level 3 degradation removal is supposed to be a level 2 filtered image g_2. Filtering is used to slice the grey levels corresponding to degradation-obscured text sections into a defined range of grey levels. The following is a description of how to identify a specific range using distinct grey levels produced from a level 2 filtered image g_2.

Let $l_1, l_2, l_3 \ldots l_k$ are sorted distinct grey levels of image g_2 partitioned into equal sized groups p_1, p_2, p_3, p_4, respectively. $l_1, l_2 \ldots l_{p_1}, l_{p_1+1}, l_{p_1+2} \ldots l_{p_2}$,

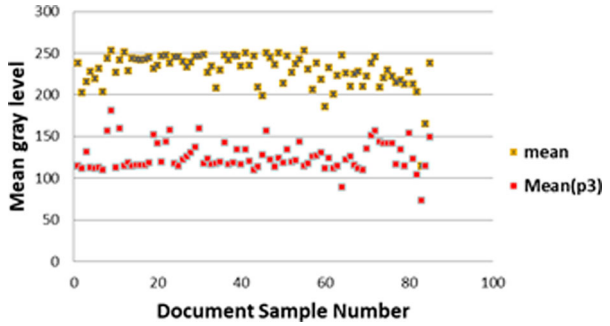

Figure 5. Mean grey level vs. mean grey level of partition 3 – DIBCO datasets.

$l_{p_2+1}, l_{p_2+2} \ldots l_{p_3}, l_{p_3+1}, l_{p_3+2} \ldots l_{p_4}$, and $l_{p_4+1}, l_{p_4+2} \ldots l_k$ represent p_1, p_2, p_3, p_4, respectively.

For each partition p_i, where $i = 1, 2, 3, 4$ are analyzed for interpretation of grey level range of degradation-obscured text sections. Figure 4 depicts the brightest grey levels (white) as the background and the textual sections as foreground darker grey levels (black) in the document image. In a grey-scale image, the darker grey levels designate the lower range, brighter grey levels designate the higher range and the midrange as degradation. Therefore, the partitions p_2 and p_3 are comprised of grey levels of degraded regions closer to textual regions. Thus, mean of grey levels of partition p_2 is employed for stain marks type degradation removal in level 3 as given by (7).

$$g_3(x,y) = \begin{cases} 255 & g_2(x,y) \geq \mu(p_2) \\ 0 & \text{Otherwise} \end{cases} \tag{7}$$

In (7), $\mu(p_2)$ represents the mean of grey levels in partition p_2 which is computed as given by (8).

$$\mu(p_2) = \frac{1}{n} \sum_{i=p_2+1}^{p_3} l_i \tag{8}$$

where n is the number of grey levels in partition p_2 ranging from $l_{p_1+1}, l_{p_1+2} \ldots l_{p_2}$ to $i = p_1 + 1, p_1 + 2, \ldots p_2$.

Figure 5 indicates the relationship between the mean grey level of gradient image G_d in level 1 and the mean grey level of partition 3 of image g_2 for all the document samples of DIBCO.

Table 3. Context of evaluation metrics.

Metric type	Context
FM	Range: 0–1 … O: OI ≈ GI ↓ 1: OI ≈ GI ↑
PFM	Range: 0–1 … O: OI ≈ GI ↓ 1: OI ≈ GI ↑
PSNR	High: OI ≈ GI ↑ Low: OI ≈ GI ↓
NRM	High: OI ≈ GI ↓ Low: OI ≈ GI ↑
DRD	High: OI ≈ GI ↓ Low: OI ≈ GI ↑
MPM	High: OI ≈ GI ↓ Low: OI ≈ GI ↑

GI → ground truth image; ↑ → high correlation; oi → obtained image; ↓ → low correlation.

Table 4. DIBCO competition datasets.

Datasets	Number of images – handwritten	Number of images – printed	No. of images with degradation-obscured text regions
DIBCO 2009	5	1	3
DIBCO 2010	10	–	–
DIBCO 2011	–	8	2
DIBCO 2012	13	1	2
DIBCO 2014	10	–	0
DIBCO 2013	8	8	4
DIBCO 2016	10	–	2
DIBCO 2017	10	10	4
DIBCO 2018	10	–	3
DIBCO 2019	5	16	2

Algorithm: pseudo_coloring(g_3, G_d)

1. Apply Otsu's thresholding on gradient G_d
Temp → Threshold (G_d)
2. Filter large objects of area greater than 500 pixels to obtain binary mask I_{ref2}
B_d → filter(Temp(area(obj(:))) > S)
3. Compute threshold
Θ → mean_graylevel ((g3)/2)
4. Maximize the discrimination range of gray levels of text sections to its obscuring degradations using a threshold k
r → number of rows (G_d)
c → number of columns (G_d)
for i = 1:r
  for j = 1:c
    if(B_d(i,j) = = 1)
      if(g_3(i,j) > = Θ)
        g_3(i,j) = max_gray level;
      end if
    else
      g_3 (i,j) = 0;
    end if
  end for
end for
5. Stop

The distribution of mean quantities applied in level 1 to level 2 shows a clear distinction, allowing for multiple degradations to be addressed at separate levels.

Table 2. Dataset details of palm leaf document images.

Sources	Place/district	Type of script/ content	Number of samples	Types of degradations – palm leaf images
Ancient Hindu temple – Kaladi mana	Kerala-Palakkad	Vedic Malayalam manuscript-Devimahathmyam	15	Brittle nature Insect activity
Ancient Brahmin Agrahara – Kaladi Mana	Kerala-Palakkad	Mythological Malayalam manuscript-kamba Ramayanam	45	Shrinking Uneven illumination
Ancient Illem – Neelamana	Kerala-Kannur	Old Ramayana Sanskrit slogas written in old Malayalam	15	Brittle nature Insect activity Fungal activity
Illem – Neelamana	Kannur	Ancient ayurvedic medicine details	15	Brittle nature, uneven illumination, brownish shades Light black shades, shrinking

Figure 6. Observer grading scale – palm leaf output evaluation.

Figure 7. Proposed model outcomes – DIBCO samples with text obscured by degradations. (1a) 2009-1, (2a) 2009-2, (3a) 2009-3, (1b) 2009-1, (2b) 2009-2, (3b) 2009-3, (4a) 2011-1, (5a) 2011-2, (6a) 2012-1, (7a) 2012-1, (4b) 2011-1, (5b) 2011-2, (6b) 2012-1, (7b) 2012-1, (8a) 2013-1, (9a) 2013-2, (10a) 2013-3, (8b) 2013-1, (9b) 2013-2, (10b) 2013-3, (11a) 2013-4, (12a) 2016-1, (13a) 2016, (11b) 2013-4, (12b) 2016-1, (13b) 2016, (14a) 2017-1, (15a) 2017-2, (16a) 2017-3, (17a) 2017-4, (14b) 2017-1, (15b) 2017-2, (16b) 2017-3, (17b) 2017-4, (18a) 2018-1, (19a) 2018-2, (20a) 2018-3, (18b) 2018-1, (19b) 2018-2, (20b) 2018-3, (21a) 2019-1, (22a) 2019-2, (21b) 2019-1, (22b) 2019-2.

3.6. Pseudo-colouring and post-enhancement

The pseudo-colouring process aims to increase the grey level discriminating range between text sections and stain type degradations. This technique is also important for restoring text strokes that have been obscured by stain degradation. This entails mapping grey levels from darker to somewhat lighter tones. In the level 3 filtered image g_3, the partial prevalence of stain mark degradations that are close to textual grey levels remains. The algorithm below depicts the process of applying pseudo-colouring.

To adjust grey levels related to stain degradations, the pseudo-colouring algorithm assumes an input of level 3 filtered image g_3 and gradient image G_d. The next step is to obtain the binary mask B_d, which contains degradation-obscured text sections. The binary mask B_d is then used for the pseudo-colouring process. The threshold that is applied to level 3 filtered picture g_3 with reference to on pixels in binary mask B_d determines the outcome of this process. According to our findings, a threshold of is determined using the 50% of the mean of grey level as provided in step 3 of the method. The threshold's implications paint a grey level at pixel g_3 (x, y) that is above the threshold Θ to maximum grey level 255 and below the threshold Θ to minimum grey level 0, as shown in step 4.

Initially, Otsu's thresholding operator T is applied to gradient image G_d, resulting in the formation of binary image B_d by assigning a pixel $G_d(x_i, y_i)$ lying above the threshold T to 1 and below T to 0. This operation will be carried out for all pixels with $i = 1, 2, 3 \ldots m$ rows and $j = 1, 2, 3 \ldots n$ columns. Further, the related components of binary image B_d are interpreted, which are a combination of text sections and degradation-obscured text sections.

If $\varkappa_1, \varkappa_2, \varkappa_3 \ldots \varkappa_p$ are the connected components, in the binary image B_d, then each connected component is subject to analysis based on its area of pixels and each $\varkappa_c$ with $c = 1, 2, 3 \ldots p$ is subject to predicate area of component $A(\varkappa_c) >= S$ pixels. The detection of text sections obscured by degradations is based on the fact that the majority of the obscured text sections have an area greater than 500 pixels. Thus, repeating the process with respect to connected components from $\varkappa_1, \varkappa_2, \varkappa_3 \ldots \varkappa_p$ would result into creation of a binary mask B_d. The mask is critical in ensuring that subsequent operations are applied only to text sections hidden by stain degradation in level 3 filtered image g_3, which correspond to pixels in binary mask B_d. This is accomplished via a threshold Θ which is mean of level 3 filtered image g_3 and multiplied by $\frac{1}{2}$.

As described in step 4 of the technique, threshold Θ is applied to those pixels in $g_3(x, y)$ that satisfy $B_d(x, y) = 1$ in binary mask B_d, which is used as a reference image for removing stain degradations that are obscuring the text sections. Each $g_3(x,y) > \Theta$ is quantized with $g_3(x, y) = 255$ and the below threshold Θ to 0 resulting in level 4 filtered image g_4. Additionally, level 4 filtered image g_4 is subject to morphological operations for enhancement of retained textual sections with the help of morphological bridging operators followed by dilation to obtain the final binarized image.

Table 5. Performance of sample observatory analysis.

Sample number	% of observers graded 1	% of observers graded 2	% of observers graded 3	% of observers graded 4	Grade based on maximum voting
Sample-1	0	8	56	36	3
Sample-2	68	32	0	0	1
Sample-3	0	0	8	92	4
Sample-4	0	0	12	88	4
Sample-5	8	44	48	0	3
Sample-6	0	0	20	76	4
Sample-7	20	76	4	0	2
Sample-8	4	36	60	0	3
Sample-9	84	16	0	0	1
Sample-10	0	4	36	60	4
Sample-11	0	92	8	0	2
Sample-12	0	100	0	0	2
Sample-13	0	4	88	8	3
Sample-14	0	0	76	24	3
Sample-15	0	4	52	44	3
Sample-16	92	8	0	0	1
Sample-17	0	0	68	48	3
Sample-18	4	88	8	0	2
Sample-19	0	0	68	32	3
Sample-20	0	0	72	28	3
Sample 21	0	24	76	0	3
Sample 22	100	0	0	0	1

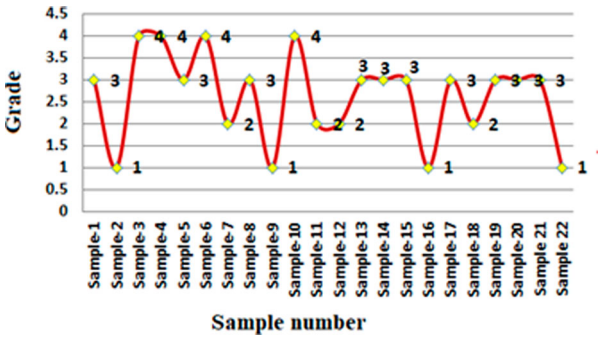

Figure 8. Grades obtained based on maximum voting.

4. Experimental analysis

Evaluation of the proposed binarization algorithm is performed on DIBCO ancient document images available with DIBCO 2009, DIBCO 2010, DIBCO 2011, DIBCO 2012, DIBCO 2013, DIBCO 2016, DIBCO 2017, DIBCO 2018, DIBCO 2019 and 55 ancient palm leaf images. To demonstrate the efficacy of the proposed model, experimental trials are predominantly conducted on documents containing concealed undertext sections. There are 125 images in the dataset, with 81 handwritten and 44 printed images. For experimental analysis, standard datasets of palm leaf of Balinese script and palm leaf datasets of Malayalam script are also used. Palm leaf Malayalam manuscripts were

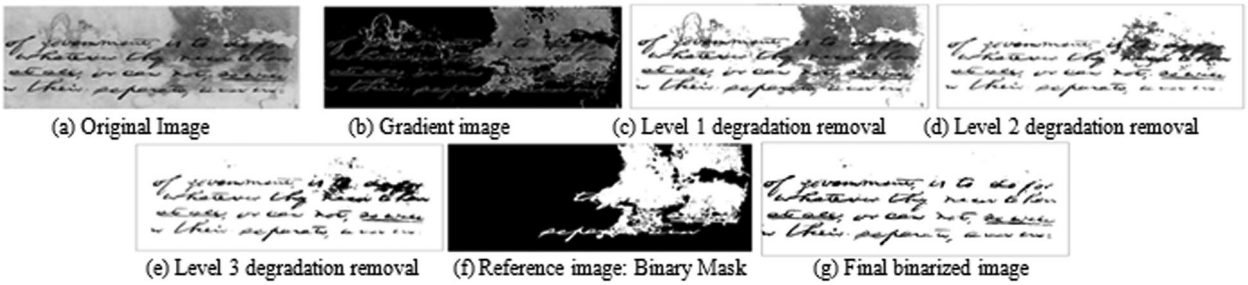

Figure 9. Proposed binarization algorithm – results presented. (a) Original Image, (b) Gradient image, (c) Level 1 degradation removal, (d) Level 2 degradation removal, (e) Level 3 degradation removal, (f) Reference image: Binary Mask, (g) Final binarized image.

Figure 10. Proposed binarization algorithm – results presented. (a) Original image, (b) Gradient image, (c) Level 1 degradation removal, (d) Level 2 degradation removal, (e) Level 3 degradation removal, (f) Binary Mask, (g) Binarized image.

obtained from various localities in the Palakkad district of Kerala. The number of samples obtained and the types of scriptures employed in palm leafs are shown in Table 2.

For up to 10 documents of Malayalam palm leaf manuscripts to be evaluated, ground truth images are created using imtool in MATLAB. The document images for experimentation are chosen with a higher degree of degradation in consideration. Validation of the remaining documents is done with the help of 25 observers using observer testing procedures. Poorly readable (P), fairly readable-partial degradations (FP-Y), fairly readable-no degradations (FP-N) and clearly readable (C) are the four levels of observer results. Figure 6 depicts the observer grading scores, with 1 being the lowest and 4 being the greatest.

The proposed model is thoroughly evaluated utilizing DIBCO competition dataset evaluation metrics

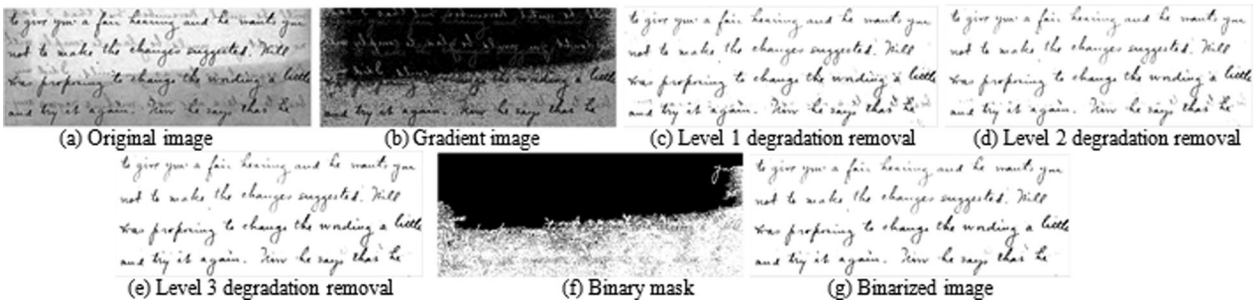

Figure 11. Evaluation of proposed algorithm towards removal of bleed/show throughs. (a) Original image, (b) Gradient image, (c) Level 1 degradation removal, (d) Level 2 degradation removal, (e) Level 3 degradation removal, (f) Binary mask, (g) Binarized image.

such as FM (F-measure), pFM (pseudo-F-measure), PSNR (peak signal noise ratio), NRM (negative rate metrics), DRD (distance reciprocal distortion) and MPM (misclassification penalty metrics) [43]. Table 3 shows the context of each metric type implying the performance of the proposed model.

The following assessment measures are used to evaluate DIBCO competition datasets, with a primary focus on images with obscured text sections, as shown in Table 4. Figure 7 displays the sample images considered in the evaluation as well as the results.

Ink bleed-through reflections from the opposite side of the paper is one sort of degradation, and as shown in Figures 7-(1b) 2009-1, (7b) 2012-1 and (12b) 2016-1, degradations that obscured text sections are successfully erased, and the qualitative grade is provided as C with a score of 4. Other degradation types, such as the stains shown in Figures 7-(2b) 2009-2, (8a) 2013-1 and (9b) 2013-2, are rated as FP-N with a qualitative score of 3, whereas degradation-obscured text in Figures 7-(9b) 2013-2, (11b) 2013-4 and (16b) 2017-3 are rated as fairly readable-partial degradations (FP-Y)

Figure 12. Outcome of proposed method versus state of art methods. (i). Sample image-1: DIBCO 2009, (a) Original Image, (b) Proposed method, (c) Niblack's,(d) Otsu, (e) Sauvola's, (f) Wolf's, (g) Kittler's method, (h) Bradley's method, (i) Local Otsu's method, (j) Gatos's method, (k) Brenson's method, (l) Feng's method. (ii). Sample image-2: DIBCO 2013, (a) Original image, (b) Proposed method, (c) Niblack's, (d) Otsu, (e) Sauvola's, (f) Wolf's, (g) Kittler's method, (h) Bradley's method, (i) Local Otsu's, (j) Gato's method, (k) Brenson's method, (l) Feng's method. (iii). Sample image-3: DIBCO 2017, (a) Original image, (b) Proposed method, (c) Niblack's, (d) Otsu, (e) Sauvola's, (f) Wolf's, (g) Kittler's method, (h) Bradley's method, (i) Local Otsu's, (j) Gato's method, (k) Brenson's method, (l) Feng's method. (iv). Sample image-4: DIBCO 2018, (a) Original image, (b) Proposed method, (c) Niblack's (d) Otsu, (e) Sauvola's (f) Wolf's, (g) Kittler's method (h) Bradley's method, (i) Local Otsu's (j) Gato's method, (k) Brenson's method (l) Feng's method. (v). Sample image-5: DIBCO 2011, (a) Original image, (b) Proposed method, (c) Niblack's, (d) Otsu's, (e) Sauvola's, (f) Wolf's, (g) Kittler's method, (h) Bradley's method, (i) Local Otsu's, (j) Gato's method, (k) Brenson's method, (l) Feng's method, (vi). Palm leaf sample image-1, (a) Original image, (b) Proposed method, (c) Niblack's, (d) Otsu's, (e) Sauvola's, (f) Wolf's, (g) Kittler's method, (h) Bradley's method, (i) Local Otsu's, (j) Gato's method, (k) Brenson's method, (l) Feng's method. (vii). Palm leaf sample image-2, (a) Original image (b) Proposed method, (c) Niblack's (d) Otsu's, (e) Sauvola's (f) Wolf's, (g) Kittler's method (h) Bradley's method, (i) Local Otsu's (j) Gato's method, (k) Brenson's method (l) Feng's method.

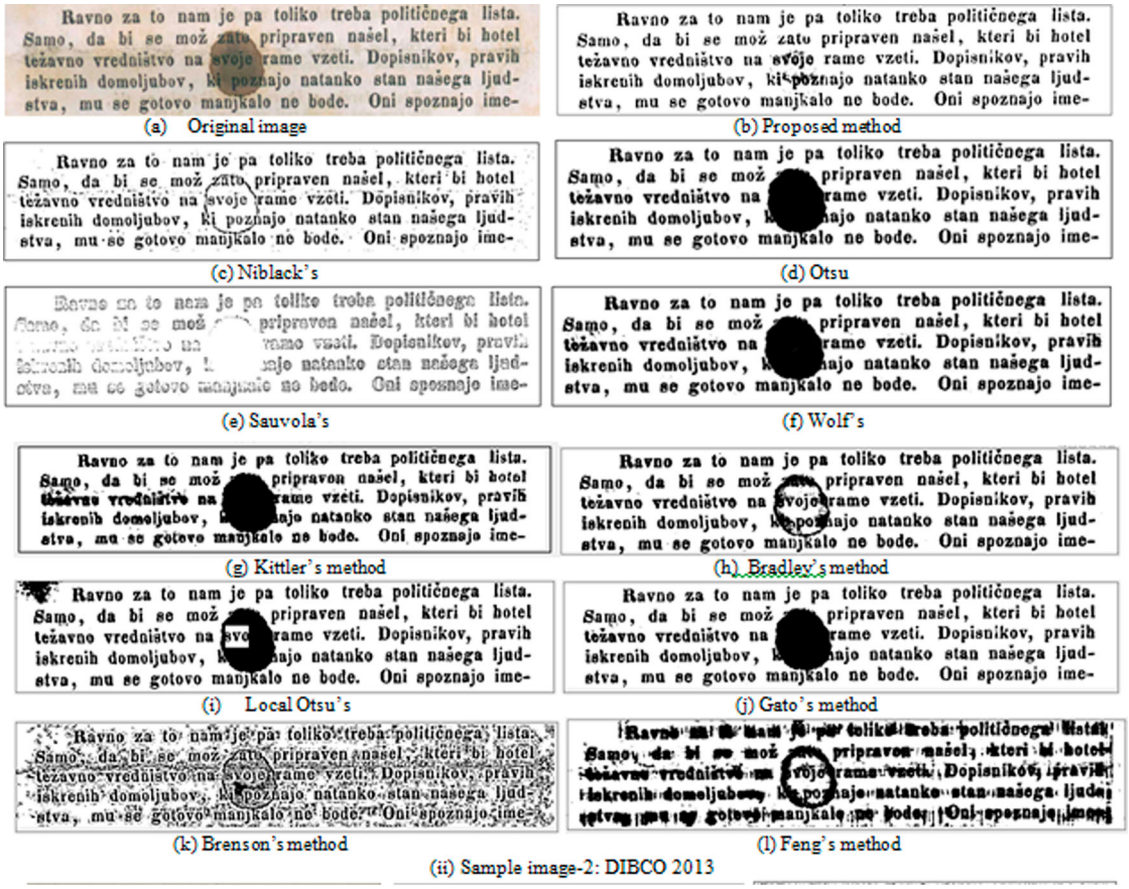

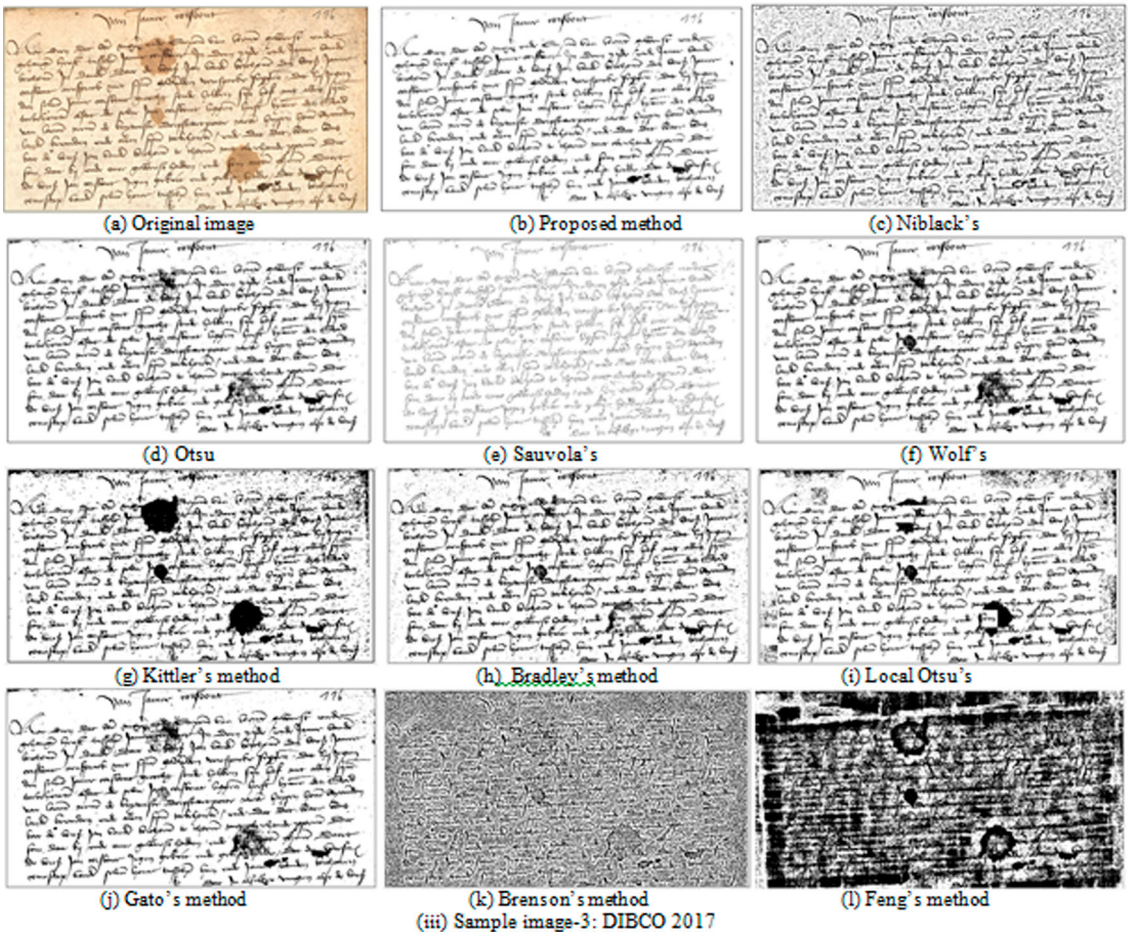

Figure 12. Contined.

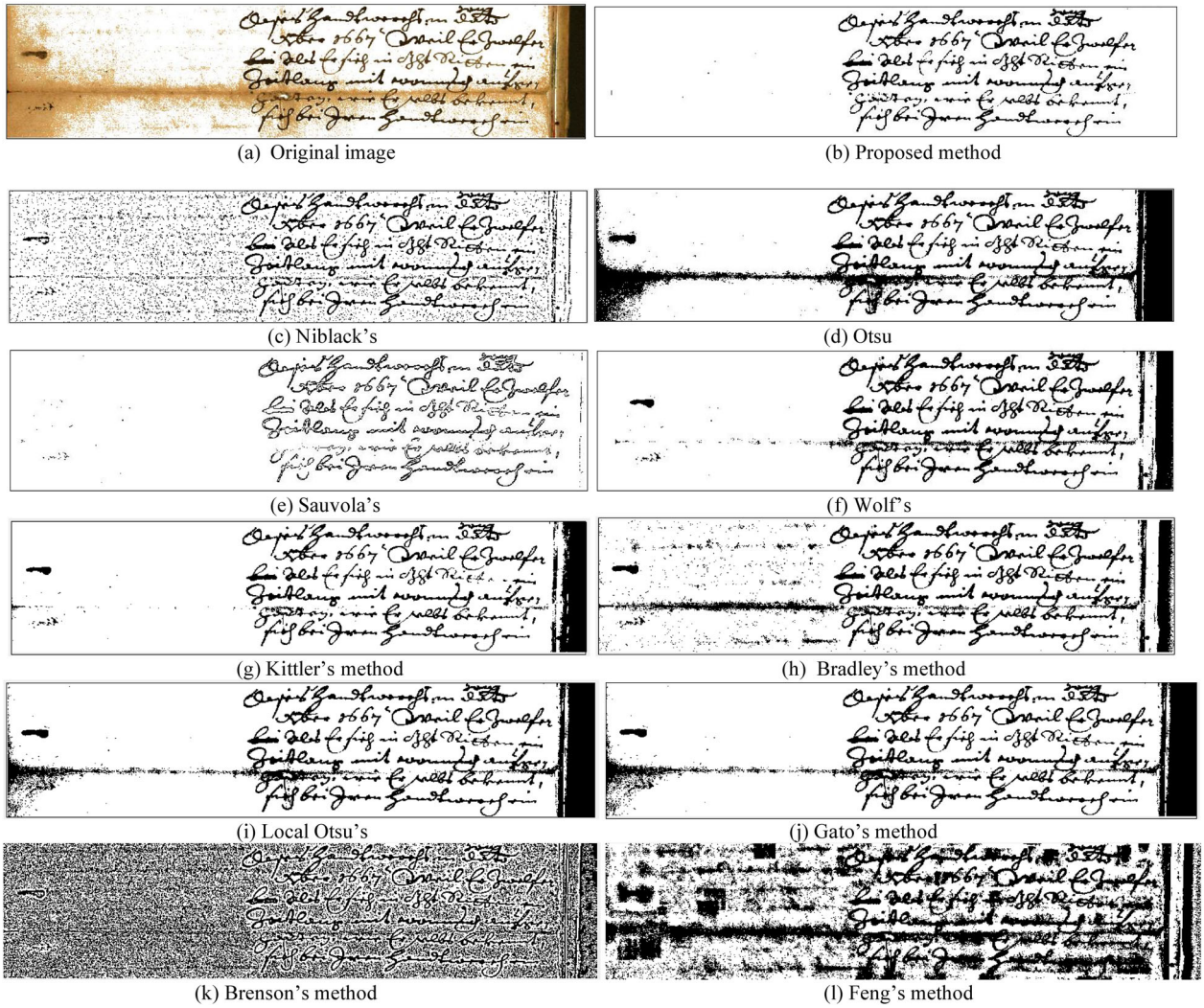

Figure 12. Contined.

with a qualitative score of 2, and Figure 7-(2b) 2012-1 is rated as 1. Degraded obscured photocopied documents (6b) 2012-1, on the other hand, have a qualitative score of 2 and are assessed as moderately readable-partial degradations (FP-Y).

Table 5 shows the results of sample observer assessment for 22 document samples, which are text sections obscured by degradations. Table 5 shows the percentage of observers who awarded each sample 1, 2, 3 or 4 rating. The percentage of observers graded as a percentage of the total number of observers is derived sample wise based on the number of observers graded as a percentage of the total number of observers. The samples are then graded using the final grade based on the highest percentage of votes. Figure 8 depicts the sample-by-sample grades based on maximum votes.

As per the subjective analysis conducted on stained degraded samples for 22 samples, 18% of observers graded the samples with the highest grade of 4, 45% of observers with a rating of 3, 18% with 2 and remaining 18% with 1 of low rating. It is inferred that the highest number of samples are binarized where the text restoration is fairly readable and partial degradations remained and only 18% are rated high indicating better visibility of obscured text sections after stain removal. Ten samples of stain degradations that are obscuring text sections are graded 3 in Table 5, indicating that the text sections have been restored by successfully removing the degradations that are obscuring text sections. Four more examples received a four rating, indicating excellent noise removal and great text retention. Four samples are scored as 2, and four samples are graded as 1, indicating a low text retention rate with partial stain degradation removal. Figures 9–11 show how the proposed technique performs on DIBCO samples that have been specially damaged by stains at different phases of the algorithm.

Figure 12 also shows the experimental results of the proposed approach with several state-of-the-art adaptive thresholding strategies. Adaptive thresholding methods which are compared include Niblack 1986 [3], Gatos et al. [4], Wolf et al. 2002 [5], Bernsen's [6], Bradley's [7], Kittler's [8], Sauvola's [9], local Otsu's [10], Feng's [27] are considered for evaluating comparative results. The results show that the proposed method, when compared to state-of-the-art

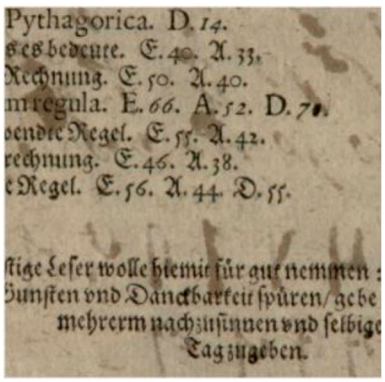
(a) Original image

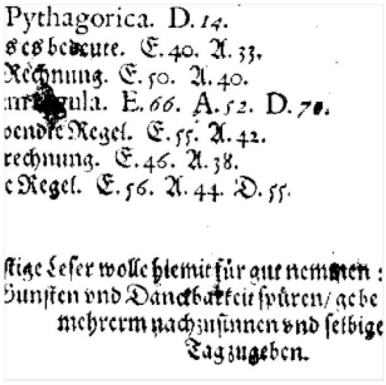
(b) Proposed method

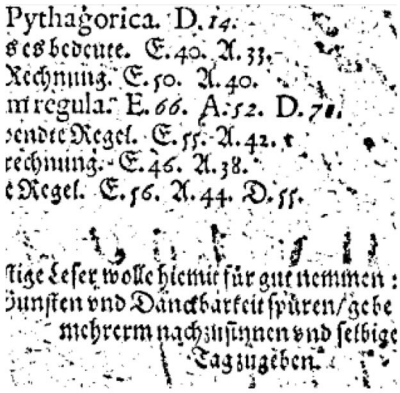
(c) Niblack's

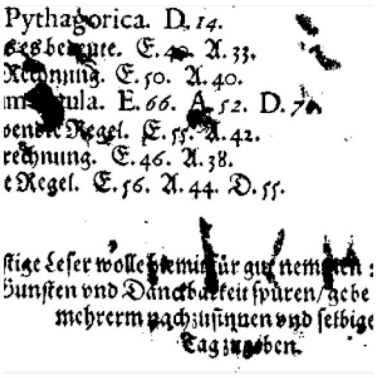
(d) Otsu's

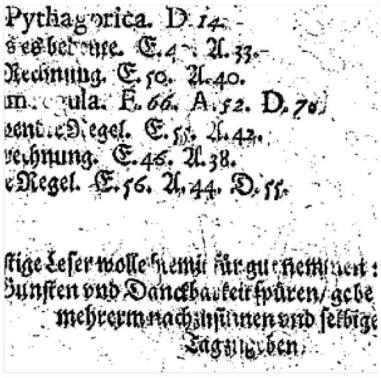
(e) Sauvola's

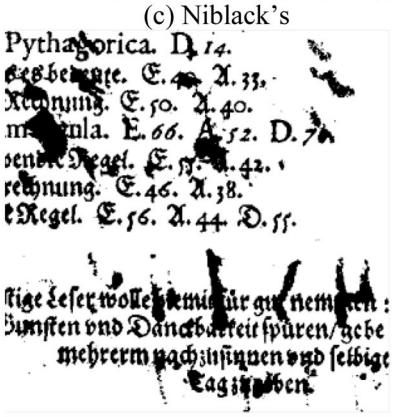
(f) Wolf's

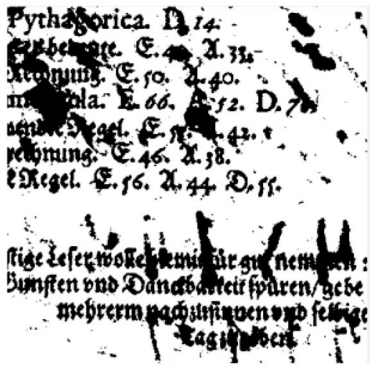
(g) Kittler's method

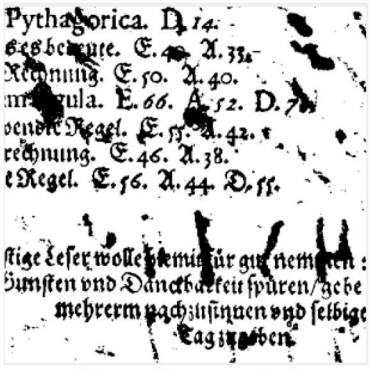
(h) Bradley's method

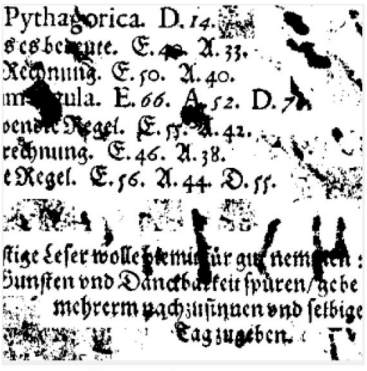
(i) Local Otsu's

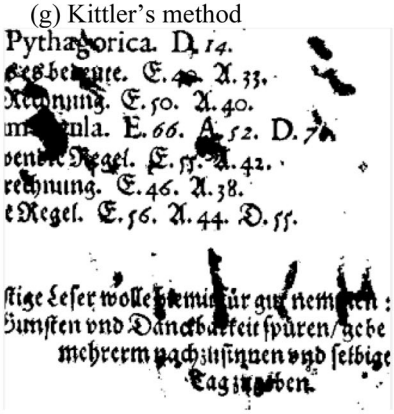
(j) Gato's method


(k) Brenson's method


(l) Feng's method

(v) Sample image-5: DIBCO 2011

Figure 12. Contined.

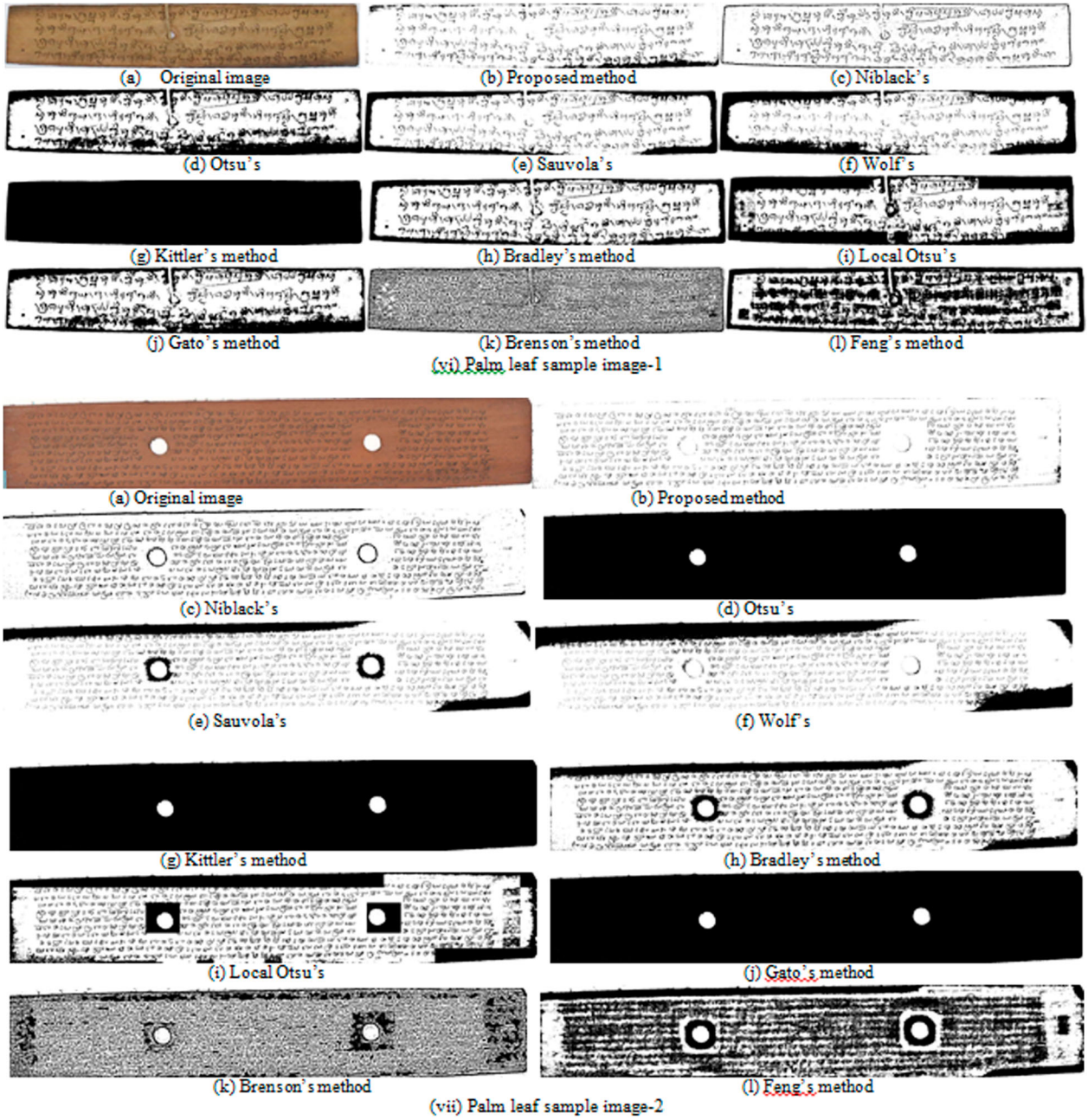

Figure 12. Contined.

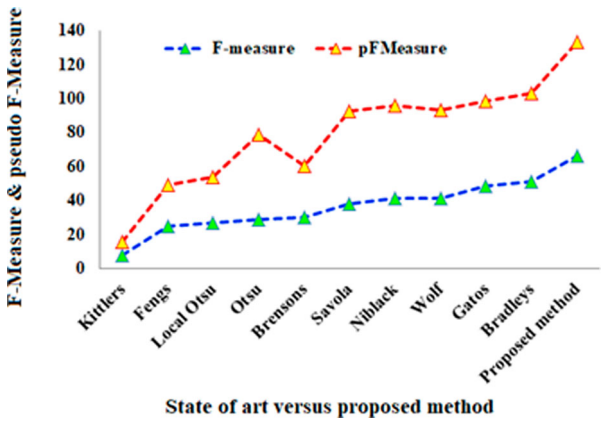

Figure 13. Evaluation outcomes – proposed algorithm vs. state of art methods – text obscured by stain degradation samples.

techniques, is capable of removing noise and retaining text that has been obscured by degradations. In addition, the proposed method outperforms state-of-the-art techniques in terms of stain removal, as shown in Figure 12. Figure 12 shows the average F-measure of stain removal of 22 samples from DIBCO datasets and its comparative results. According to our findings, whilst the proposed technique for noise removal achieves satisfactory results for palm leaf enhancement, it causes text breakages in palm leaf documents. Furthermore, all existing methods for noise removal in palm leaf manuscripts have failed, with the exception of the Niblack method, which performs similarly to the proposed method. Furthermore, when applied to stained degradation samples of DIBCO datasets,

Table 6. Evaluation of *F*-measure on DIBCO 2009, 2010, 2011, 2012, 2013 datasets – existing versus proposed techniques.

Method	Performance metrics	DIBCO 2009	DIBCO 2010	DIBCO 2011	DIBCO 2012	DIBCO 2013	DIBCO 2014	DIBCO 2016
F-measure	Proposed method	71.91	72.29	67.62	10.76	11.35	12.51	79.08
	Sauvola	70.49	69.66	64.04	12.88	7.58	11.24	53.20
	Local Otsu	44.49	73.24	63.59	12.10	9.36	18.73	77.68
	Bradleys	64.37	100	17.90	0.65	0.69	0.30	17.25
	Brensons	71.11	57.20	67.07	11.16	9.77	16.60	75.46
	Fengs	62.79	52.78	61.04	19.69	15.06	19.08	67.76
	Otsu	55.25	67.10	61.86	8.087	7.268	11.14	70.50
	Kittlers	70.49	69.66	63.59	12.88	7.58	11.24	71.98
	Wolf	71.60	72.48	67.53	10.84	8.86	12.99	76.73
	Gatos	73.06	67.33	68.54	11.92	12.05	41.38	73.11
	Niblack's	50.79	56.53	54.72	12.16	10.02	11.92	64.00
PSNR	Proposed method	11.68	14.13	11.77	10.68	9.59	9.30	13.20
	Sauvola	11.53	15.00	12.45	10.20	9.49	9.42	12.65
	Local Otsu	9.58	12.91	12.27	10.12	9.15	8.69	9.68
	Bradleys	13.30	11.60	11.07	11.69	11.30	10.29	15.79
	Brensons	11.76	11.65	11.61	10.63	9.86	9.04	12.39
	Fengs	7.69	6.72	6.43	8.50	8.50	8.28	9.17
	Otsu	11.52	14.11	11.23	10.76	9.92	9.51	15.98
	Kittlers	11.53	15.00	12.27	10.20	9.49	9.42	11.37
	Wolf	11.97	14.44	12.10	10.71	9.69	9.37	13.02
	Gatos	5.89	4.94	5.61	5.65	6.40	4.83	4.95
	Niblack's	9.21	13.36	11.37	9.83	9.06	8.99	12.1
NRM	Proposed method	0.22	0.22	0.25	0.47	0.49	0.48	0.10
	Sauvola	0.23	0.24	0.27	0.48	0.50	0.48	0.34
	Local Otsu	0.36	0.22	0.27	0.47	0.50	0.47	0.18
	Bradleys	0.25	0.10	0.44	0.49	0.50	0.49	0.45
	Brensons	0.23	0.18	0.25	0.47	0.49	0.47	0.21
	Fengs	0.32	0.24	0.35	0.49	0.49	0.48	0.28
	Otsu	0.31	0.26	0.28	0.48	0.49	0.48	0.22
	Kittlers	0.23	0.24	0.27	0.48	0.50	0.48	0.24
	Wolf	0.22	0.22	0.25	0.47	0.49	0.47	0.20
	Gatos	0.26	0.29	0.30	0.46	0.48	0.47	0.25
	Niblack's	0.35	0.31	0.32	0.48	0.50	0.48	0.27
DRD	Proposed method	19.54	1018.08	17.78	26.56	25.77	24.91	30.52
	Sauvola	28.14	895.47	14.77	33.15	29.59	23.90	51.38
	Local Otsu	43.16	1109.24	17.37	31.26	33.43	30.59	78.24
	Bradleys	12.04	0	19.49	19.59	18.41	23.54	7.90
	Brensons	19.64	761.12	20.19	27.14	25.23	27.30	36.18
	Fengs	60.96	2285.81	81.068	48.04	35.10	33.94	86.77
	Otsu	22.61	870.57	21.94	25.85	22.29	23.13	31.09
	Kittlers	28.14	895.47	17.37	33.15	29.59	23.90	43.96
	Wolf	17.30	861.51	15.9694	26.50	24.61	24.55	32.06
	Gatos	94.32	10236.6	93.82	103.44	60.64	85.20	235.75
	Niblack's	46.13	3516.43	22.81	33.43	29.22	26.38	52.52
MPM	Proposed method	5.9837143395	13.08285	11.35308447	11.19298	16.39978	15.41481	7.379354
	Sauvola	11.845998	10.02953	11.395146	35.3612	33.57677	13.63463	8.881051
	Local Otsu	23.091908	19.24747	20.34821	15.71389	39.89043	28.24012	27.02578
	Bradleys	11.472759	10.23	24.477369	11.98204	12.870354	17.927489	7.102112
	Brensons	9.188106	12.94921	19.527270	12.59077	17.42683	22.13212	11.26289
	Fengs	84.240831	63.38222	119.157560	48.49074	39.30045	41.10093	61.30257
	Otsu	8.544304	17.99541	20.735447	10.84983	13.27856	12.97212	7.62989
	Kittlers	11	10.02	20.34	35.36	33.57	13.63	12.71
	Wolf	5.050494	12.8329	10.540107	11.55354	15.29663	15.08265	7.519753
	Gatos	81.901358	182.687	104.651355	118.5249	80.58204	122.116	102.07
	Niblack's	49.319682	26.87155	20.7184836	27.1714	30.65412	21.93915	33.16636

the results of state-of-the-art methods for eliminating degradations obscuring text sections are unsuccessful since text sections are corroded together with stain removal.

The visual results of Figure 12 and the quantitative evaluation of the same in Figure 13 clearly show that the proposed method outperforms the state-of-the-art methods in stain removal. F-measure and pFM had the greatest values of 66 and 67.31 by the proposed method and the lowest values of 7.84 and 7.99 by Kittlers method. Furthermore, quantitative analysis is performed on all DIBCO datasets from 2009 to 2019 as well as palm leaf manuscripts in Balinese and Malayalam, and performance measures such as F-measure, PSNR, NRM, DRD and MPM are listed in Tables 6 and 7. The greatest F-measure will be close to 1, indicating that the binarization technique is effective, and the NRM and MPM values will be close to zero, indicating that the algorithm is reliable in classifying pixels into background and foreground.

Figures 14 and 15 show the quantification of results produced in terms of MPM for all DIBCO and palm leaf datasets using the proposed method vs state-of-the-art techniques. Figure 13 depicts the tradeoff between the DIBCO 2009–2014 datasets and MPM, revealing that the proposed method and Sauvola have the lowest MPM of all known methods. Figure 15 shows the MPM of the proposed technique and state-of-the-art

Table 7. Evaluation of *F*-measure on DIBCO 2017, 2018, 2019 and palm leaf datasets – existing versus proposed techniques.

Metrics	Methods	DIBCO 2017	DIBCO 2018	DIBCO 2019A	DIBCO 2019B	PALM LEAF-balinese	PALM LEAF – Malayalam
F-measure	Proposed method	71.52	64.55	72.42	66.17	33.30	58.94
	Sauvola	74.59	64.68	60.21	60.26	20.94	29.32
	Local Otsu	80.06	75.60	64.56	47.29	20.94	27.52
	Bradleys	66.76	93.39	70.76	83.42	3.00	40.22
	Brensons	75.91861	66.09308	66.2709	70.75118	15.83309136	78.69475318
	Fengs	63.31645	52.51703	60.45278	64.92845	26.55494401	72.66579078
	Otsu	59.61972	50.03915	63.09165	80.33765	13.18495421	60.94963311
	Kittlers	77.28376	75.39058	60.21457	60.2683	20.94908869	29.32939734
	Wolf	74.03913	66.98195	75.53972	64.29816	10.33142899	60.06385895
	Gatos	77.22104	74.81333	58.98279	66.8301	30.23721728	59.50053431
	Niblack's	64.51383	61.46351	57.29345	77.07415	29.34178548	70.93898219
PSNR	Proposed method	14.19057	14.25518	10.3396	7.750958	7.378783	9.19112
	Sauvola	13.98961	10.38885	12.96286	3.284595	3.351877	2.058136
	Local Otsu	10.02776	10.35584	11.82337	2.121085	3.351877	2.714315
	Bradleys	14.63577	17.36689	11.31665	7.984267	10.8468	11.5091
	Brensons	11.37081	12.82323	11.14071	8.405088	7.960028	10.0611
	Fengs	7.685329	10.18957	7.521082	7.325468	7.329124	8.768151
	Otsu	14.2183	14.58467	11.32997	16.87789	9.993971	2.238994
	Kittlers	11.81484	9.51317	12.96286	3.284595	3.351877	2.058136
	Wolf	12.48861	12.29307	10.22018	8.588232	8.243797	10.22399
	Gatos	6.168472	6.195984	3.145769	5.214471	5.811735	7.11967
	Niblack's	11.53853	9.849303	10.83335	8.3387	5.176138	7.762337
NRM	Proposed method	0.238616	0.256253	0.243171	0.300647	0.526817	0.329806
	Sauvola	0.222628	0.275769	0.292601	0.323553	0.512157	0.476125
	Local Otsu	0.181018	0.220611	0.275399	0.352952	0.512157	0.470323
	Bradleys	0.183991	0.087545	0.148158	0.136423	0.505741	0.415106
	Brensons	0.209522	0.258554	0.276026	0.265901	0.508912	0.196316
	Fengs	0.323201	0.35714	0.345763	0.318017	0.490297	0.251452
	Otsu	0.306872	0.33802	0.289169	0.144914	0.485258	0.235984
	Kittlers	0.199712	0.222931	0.292601	0.323553	0.512157	0.476125
	Wolf	0.21399	0.241557	0.210173	0.301592	0.519918	0.310681
	Gatos	0.219892	0.249775	0.378174	0.326406	0.502988	0.355534
	Niblack's	0.27349	0.297693	0.324484	0.221233	0.533159	0.270815
DRD	Proposed method	2195.655	47.95631	438.8607	28.86234	65.91742	29.96106
	Sauvola	1922.538	113.6091	272.9274	89.18531	231.013	151.8387
	Local Otsu	12339.77	156.7995	672.6539	108.8852	231.013	140.7843
	Bradleys	3.192968	3.832793	2.210127	7.09321	19.02961	33.77319
	Brensons	8616.7	68.52243	339.1229	21.98865	50.88137	23.11759
	Fengs	36212.58	149.5125	610.2073	28.26136	58.93159	31.21009
	Otsu	2063.27	50.78871	331.6965	2.035868	26.24063	76.5307
	Kittlers	6454.803	142.9923	272.9274	89.18531	231.013	151.8387
	Wolf	2325.866	47.4465	458.7864	21.15291	48.62103	21.32213
	Gatos	27093.59	278.4171	2221.351	56.12331	91.23314	41.95481
	Niblack's	3686.407	114.1995	1105.902	40.01681	113.1953	40.49939
MPM	Proposed method	17.56277	16.23767	47.97877	23.18777	97.76475	58.65631
	Sauvola	15.7349	84.28823	17.10269	83.30992	303.4943	404.2385
	Local Otsu	37.27853	94.66958	32.70495	142.6001	303.4943	370.8748
	Bradleys	0.251689	0.109939	1.124968	8.375522	25.17536	81.70138
	Brensons	27.22406	32.99723	32.93929	18.99129	74.25224	46.16735
	Fengs	86.99323	47.83302	89.40533	43.57811	71.66141	80.16943
	Otsu	13.64987	9.313822	29.37483	1.647606	21.9467	197.6948
	Kittlers	22.78	84.86296	17.10269	83.30992	303.4943	404.2385
	Wolf	17.19866	28.52867	40.54497	17.19273	70.1615	40.68053
	Gatos	109.3696	104.7986	227.937	135.8741	128.2138	79.32065
	Niblack's	35.18557	65.09585	52.29313	54.91382	178.5901	95.70329

methods with respect to DIBCO 2017–2019 and palm leaf datasets in Balinese and Malayalam.

Regardless of the type of degradation, we can conclude from our quantitative investigation, which used dataset-wise averaged measures that the proposed methodology performs nearly as well as state-of-the-art techniques such as Gatos, Niblack and Wolf in varied circumstances. Other algorithms' failures can be attributed to a variety of issues, such as Otsu's technique's use of a unified threshold, which may fail to interpret the margin of difference between minute grey level changes in degraded sections of the document. Other adaptive thresholding approaches, such as Feng, Bernson, Bradley, Kittler and Local Otsu, rely on specified parameters, resulting in the higher text to non-text misclassification penalties and vice versa.

These methods are more effective in dealing with larger grey level variations in cases of uneven illuminations, show throughs and other ageing changes, but they are less effective in removing stained degradations by maintaining text sections. Gatos, Niblack, Wolf and Sauvola outperform the proposed technique in a few F-measure and PSNR cases. However, the F-measure and pFM results for the 22 samples of stained degradations that are obscuring the text sections, viz. Figure 13, show that the proposed approach is adequate. In the instances of Sauvola, Niblack, Bernson

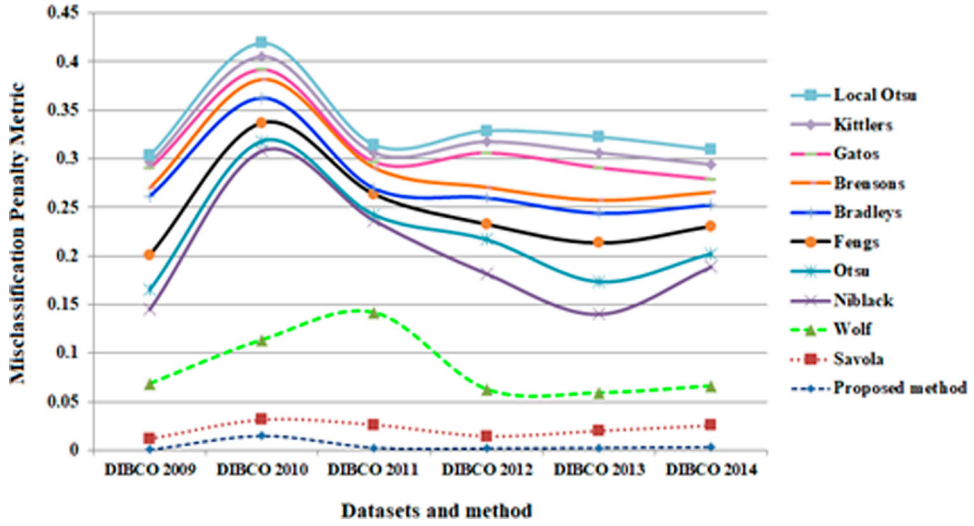

Figure 14. MPM of proposed and state of art methods versus DIBCO 2009–2014 datasets.

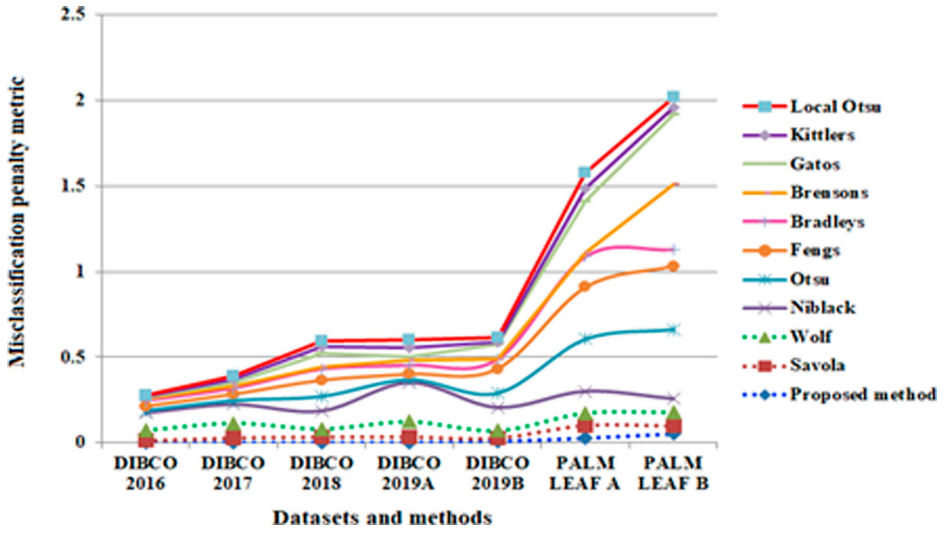

Figure 15. MPM of proposed and state of art methods versus DIBCO 2016–2019 and palm leaf datasets.

Figure 16. Exceptions of proposed algorithm.

and Gatos, we could see in Figure 11 that there were times when characters would fade along with the noise.

The removal of stained degradation by state-of-the-art also results in an unacceptably sharp transition from stained to the text section. When it comes to noise reduction from DIBCO and palm leaf documents, Otsu, Local Otsu and Kittler's are the examples where inadequate efficiency is perceived.

Following that, it is discovered that the proposed approach and Niblack perform similarly well in terms of noise removal in palm leaf documents, whereas Sauvola, Wolf and Gatos perform well in terms of DIBCO datasets. However, they fail to eliminate text breakages and noise in Balinese and Malayalam palm leaf writings. Furthermore, the suggested method fails to binarize papers with thin pen strokes, despite the fact that it reduces noise regardless of DIBCO or palm leaf documents, as shown in Figure 16. The difficulty of improving text legibility in palm leaf manuscripts, on the other hand, deserves more research.

However, as demonstrated in Figure 16, the proposed technique's efficiency for palm leaf document enhancement is not as promising as it is for DIBCO document images. Text strokes of varying lengths and show throughs with grey levels equal to the original text result in poor text stroke preservation in documents, as seen in Figure 16.

The average F-measure for the DIBCO dataset is 65.73, whilst the average F-measure for palm leaf document samples is 55.24, according to Table 5. The results show that the proposed technique is capable of removing stains, non-uniform illuminations, foxing, ageing marks and pen scribbles. For DIBCO document images, the proposed method has produced encouraging results, with an F-measure of more than 65 percent for 4 out of 10 documents and 2 out of 10 for palm leaf document images.

5. Conclusion and future work

With the application of adaptive thresholding methods, binarization of ancient degraded document images is becoming more common. Complex degradation, on the other hand, is still a mystery, despite the fact that a model based on a combination of global and local thresholding procedures generates outstanding results. To solve the degrading obscured text sections, we use a tri-level semi-adaptive binarization technique in this research. Gradient images made with RGB channels of scanned documents are significantly used in the identification of binary mask highlighting stains. Adapting the usage of thresholds to binarize deteriorating hidden text sections of the original image introduces the nature of applying local thresholds. The proposed study uses global thresholding approaches to remove level-wise degradation, whereas the post-enhancement procedure uses local thresholding techniques. Though the evaluation demonstrates that noise removal and text retention are effective for DIBCO samples, future study will be hampered by the low text retention rate for palm leaf document samples. Furthermore, the topic of the recommended algorithm's speed in comparison to other ways could be studied as a separate research challenge in the future.

Disclosure statement

No potential conflict of interest was reported by the author(s).

Funding

This research did not receive any specific grant from funding agencies in the public, commercial or not-for-profit sectors.

References

[1] Otsu N. A threshold selection method from gray level histogram, IEEE Trans Syst Man Cybernet. 1979;19(1):62–66. DOI:10.1109/TSMC.1979.4310076.
[2] Terras, Mellisa M The rise of digitization. In: Digitization perspectives. Sense Publishers; 2011. p. 3–20.
[3] Niblack W. An introduction to digital image processing. Englewood Cliffs (NJ): Prentice-Hall; 1986.
[4] Gatos B, Pratikakis I, Perantonis SJ. Adaptive degraded document image binarization. Pattern Recognit. 2006; 39(3):317–327. DOI:10.1016/j.patcog.2005.09.010.
[5] Wolf Christian, Jolion JM, Chassaing F. Text localization, enhancement and binarization in multimedia documents. In: Object recognition supported by user interaction for service robots. Vol. 2. IEEE; 2002. p. 1037–1040. DOI:10.1109/ICPR.2002.1048482.
[6] Bernsen J. Dynamic thresholding of gray-level images. In: Proceedings of the 8th international conference pattern recognition, Paris; 1986.
[7] Bradley D, Roth G. Adaptive thresholding using the integral image.
[8] Kittler J, Illingworth J. Minimum error thresholding. Pattern Recognit. 1886;19(1):41–47.
[9] Sauvola J, Pietikainen M. Adaptive document image binarization. Pattern Recognit. 2000;33(2):225–236. DOI:10.1016/S0031-3203(99)00055-2.
[10] Moghaddam RF, Cheriet M. Adotsu: an adaptive and parameterless generalization of Otsu's method for document image binarization. Pattern Recognit. 2012;45(6):2419–2431.
[11] Sauvola J, Pietikainen M. Adaptive document image binarization. Pattern Recognit. 2000;33:225–236.
[12] Lipiński AJ, Lipiński S. Binarizing water sensitive papers – how to assess the coverage area properly? Crop Protect. 2020;127:104949. DOI:10.1016/j.cropro.2019.104949.
[13] Gupta D, Bag S. A local-to-global approach for document image binarization. In: Computational intelligence in pattern recognition. Singapore: Springer; 2020. p. 693–702. DOI:10.1007/978-981-13-9042-5_60.
[14] Michalak H, Okarma K. Robust combined binarization method of non-uniformly illuminated document images for alphanumerical character recognition. Sensors. 2020;20(10):2914. DOI:10.3390/s20102914.

[15] Michalak H, Okarma K. Optimization of degraded document image binarization method based on background estimation. Journal of WSCG. 2020;28(1–2): 89–98. DOI:10.24132/CSRN.2020.3001.11.
[16] Michalak, H., & Okarma, K. Application of multilayered thresholding based on stack of regions for unevenly illuminated industrial images. In: Advanced, contemporary control. Cham: Springer; 2020. p. 773–784; DOI:10.1007/978-3-030-50936-1_65.
[17] Alexander TJ, Kumar SS. A novel binarization technique based on whale optimization algorithm for better restoration of palm leaf manuscript. J Ambient Intell Humaniz Comput. 2020: 1–8. DOI:10.1007/s12652-020-02546-2.
[18] Krupiński R, Lech P, Okarma K. Improved two-step binarization of degraded document images based on Gaussian mixture model. In: International conference on computational science. Cham: Springer; 2020. p. 467–480; DOI:10.1007/978-3-030-50426-7_35.
[19] Huang X, et al. Binarization of degraded document images with global-local U-nets. Optik (Stuttg). 2019;203:164025. DOI:10.1016/j.ijleo.2019.164025.
[20] Yang Y, Yan H. An adaptive logical method for binarization of degraded document images. Pattern Recognit. 2000;33(5):787–807. DOI:10.1016/S0031-3203(99)00094-1.
[21] Zhang X, He C, Guo J. Selective diffusion involving reaction for binarization of bleed-through document images. Appl Math Model. 2020;81:844–54. DOI:10.1016/j.apm.2020.01.020.
[22] Kaur A, Rani U, Josan GS. Modified Sauvola binarization for degraded document images. Eng Appl Artif Intell. 2020;92(March):103672. DOI:10.1016/j.engappai.2020.103672.
[23] Guo J, He C, Zhang X. Nonlinear edge-preserving diffusion with adaptive source for document images binarization. Appl Math Comput. 2019;351:8–22. DOI:10.1016/j.amc.2019.01.021.
[24] Calvo-Zaragoza J, Gallego AJ. A selectional auto-encoder approach for document image binarization. Pattern Recognit. 2019;86:37–47.
[25] Calvo-Zaragoza J, Vigliensoni G, Fujinaga I. Pixel-wise binarization of musical documents with convolutional neural networks. In 2017 Fifteenth IAPR international conference on machine vision applications (MVA), 2017. IEEE; p. 362–365.
[26] Saddami K, Munadi K, Away Y, et al. Effective and fast binarization method for combined degradation on ancient documents. Heliyon. 2019;5(10):e02613. DOI:10.1016/j.heliyon.2019.e02613.
[27] Feng S. A Novel variational model for noise robust document image binarization. Neurocomputing. 2019; 325:288–302. DOI:10.1016/j.neucom.2018.09.087.
[28] Zhao J, et al. Document image binarization with cascaded generators of conditional generative adversarial networks. Pattern Recognit. 2019;96:106968. DOI:10.1016/j.patcog.2019.106968.
[29] Sehad A, Chibani Y, Hedjam R, et al. Gabor filter-based texture for ancient degraded document image binarization. Pattern Anal Appl. 2019;22(1):1–22. DOI:10.1007/s10044-018-0747-7.
[30] Hangarge, Veershetty C, Mallikarjun. 43 Data analytics and learning; 2019. Singapore: Springer. http://link.springer.com/10.1007/978-981-13-2514-4.
[31] Xiong W, et al. Degraded historical document image binarization using local features and support vector Machine (SVM). Optik (Stuttg). 2018;164:218–23. DOI:10.1016/j.ijleo.2018.02.072.
[32] Vo QN, Kim SH, Yang HJ, et al. Binarization of degraded document images based on hierarchical deep supervised network. Pattern Recognit. 2018;74:568–586. DOI:10.1016/j.patcog.2017.08.025.
[33] Chen Y, Wang L. Broken and degraded document images binarization. Neurocomputing. 2017;237: 272–280. DOI:10.1016/j.neucom.2016.12.058.
[34] Mitianoudis N, Papamarko N. Document image binarization using local features and Gaussian mixture modeling. Image Vis Comput. 2015;38:33–51. DOI:10.1016/j.imavis.2015.04.003.
[35] Ntirogiannis K, Gatos B, Pratikaki I. A combined approach for the binarization of handwritten document images. Pattern Recognit Lett. 2014;35(1):3–15. DOI:10.1016/j.patrec.2012.09.026.
[36] Wen J, Li S, Sun J. A new binarization method for non-uniform illuminated document images. Pattern Recognit. 2013;46(6):1670–1690. DOI:10.1016/j.patcog.2012.11.027.
[37] Su B, Lu S, Tan CL. Robust document image binarization technique for degraded document images. IEEE Trans Image Process. 2013;22(4):1408–1417. DOI:10.1109/TIP.2012.2231089.
[38] Chiu YH, et al. Parameter-free based two-stage method for binarizing degraded document images. Pattern Recognit. 2012;45(12):4250–4262. DOI:10.1016/j.patcog.2012.02.023.
[39] Hedjam R, Moghaddam RF, Cheriet M. A spatially adaptive statistical method for the binarization of historical manuscripts and degraded document images. Pattern Recognit. 2011;44(9):2184–2196. DOI:10.1016/j.patcog.2011.02.021.
[40] Bataineh B, Abdullah SNHS, Omar K. An adaptive local binarization method for document images based on a novel thresholding method and dynamic windows. Pattern Recog Lett. 2017;32(14):1805–1813. DOI:10.1016/j.patrec.2011.08.001.
[41] Farrahi Moghaddam R, Cheriet M. A multi-scale framework for adaptive binarization of degraded document images. Pattern Recognit. 2010;43(6):2186–2198. DOI:10.1016/j.patcog.2009.12.024.
[42] Gatos B, Ntirogiannis K, Pratikakis I. ICDAR 2009 document image binarization contest (DIBCO 2009). In: 2009 10th International conference on document analysis and recognition. IEEE; 2019. p. 1375–1382. DOI:10.1007/s10032-010-0115-7.
[43] Puniani S, Arora S. Performance evaluation of image enhancement techniques. Int J Sig Process Image Process Pattern Recogn. 2015;8(8):251–262.